International Journal of Nanomedicine

Dovepress
open access to scientific and medical research

Open Access Full Text Article

ORIGINAL RESEARCH

Application Study of Novel Eggshell/Ag Combined with Pit and Fissure Sealants

Xiaoyu Huang[1,2], Ming Zhang[1,3], Lin Chang[1,2], Dali Zheng[2], Wei Lin[4], Yan Feng[1,2], Youguang Lu[1,2]

[1]Department of Preventive Dentistry, School and Hospital of Stomatology, Fujian Medical University, Fuzhou, Fujian Province, People's Republic of China; [2]Fujian Key Laboratory of Oral Diseases, School of Stomatology, Fujian Medical University, Fuzhou, Fujian Province, People's Republic of China; [3]Department of Conservative and Endodontic Dentistry, School and Hospital of Stomatology, Fujian Medical University, Fuzhou, Fujian Province, People's Republic of China; [4]College of Chemistry, Fuzhou University, Fuzhou, Fujian Province, People's Republic of China

Correspondence: Youguang Lu, Tel +86-591-83736429, Fax +86-591-83720599, Email fjlyg63@fjmu.edu.cn; Yan Feng, Tel/Fax +86-591-22862632, Email fengyan@fjmu.edu.cn

Objective: The study aims to enhance the anti-caries performance of pit and fissure sealants through the synthesis of novel silver nanocomposites, and to evaluate their mechanical properties and biological safety in vitro and in vivo.

Methods: The antibacterial properties of synthetic eggshell/Ag were detected by bacterial inhibition zone, minimum bacteriostatic concentration, fluorescence staining and scanning electron microscopy. The synthetic products were then combined with pit and fissure sealants to prepare specimens, and their effects on mechanical properties, antibacterial properties and cytotoxicity were evaluated. Furthermore, an oral mucosal contact model of golden hamsters was established according to the ISO10933 standard to evaluate local stimulation and systemic effects.

Results: The novel nanocomposite eggshell/Ag was confirmed to exhibit strong broad-spectrum antibacterial activity, and that the eggshell/Ag-modified pit and fissure sealant had strong antibacterial properties against common dental caries bacterial biofilms, without any significant change in mechanical properties. The gradient dilution extract showed acceptable cytotoxicity, and in the golden hamster oral contact model, there were no visible abnormalities in local mucosal tissues, blood indices, or liver and kidney histopathology.

Conclusions: These findings suggest that eggshell/Ag combined with pit and fissure sealants has strong antibacterial activity and excellent biosafety in vitro and in vivo, making it a promising candidate for clinical applications.

Keywords: silver nanocomposites, antibacterial, pit and fissure sealants, biosafety

Introduction

According to the recently published Global Burden Disease (GBD), untreated caries of permanent teeth is the most prevalent health condition worldwide, affecting nearly 2.3 billion people.[1,2] The prevalence of caries among deciduous teeth is also high, with 46.9% occurring in children aged 1 to 4 years, and 39.3% occurring in children aged 5 to 9 years.[3,4] A recent study published in August 2018, the Fourth National Oral Health Epidemiological Survey,[5] showed that the prevalence of caries among children in China is on the rise, with 71.9% in the 5-year-old age group (average caries is 4.24) and 38.5% in the 12-year-old age group (average caries is 0.86). In adolescents, 90% of caries occur in the pit and fissure.[6] To address this issue, pit and fissure sealants have been recommended to children and adolescents, as they are recognized as safe and effective in preventing and arresting the progression of caries by the American Dental Association (ADA) and the Cochrane Library.[7–9]

Adhesive sealants are commonly applied to deep pits and fissures to prevent bacterial growth and reproduction, which can lead to tooth erosion due to their metabolism and acid production. Among these sealants, photocured bisphenol-A diglycidyl methacrylate (BisGMA) resin is widely used due to its superior physical properties such as good fluidity and wettability.[10] However, resin-based materials are not without challenges,[11] including biofilm accumulation[12] and micro-leakage at the sealant edge, which can provide channels for new bacterial invasion.[13,14] Therefore, sealants with

Received: 19 January 2023
Accepted: 19 April 2023
Published: 1 June 2023

antibacterial properties are important for preventing residual bacterial proliferation and destruction in the microenvironment, as well as inhibiting subsequent bacterial adhesion to the tooth surface. This represents a significant clinical benefit for preventing dental caries.

The emergence of antibiotic resistance has posed a significant challenge in the pharmaceutical and biomedical fields, leading scientists to explore the potential of nanomaterials in combating multidrug-resistant (MDR) pathogens. Metallic nanomaterials, such as silver,[15] zinc oxide,[16] and titanium dioxide,[17] have gained significant attention as potential agents in the development of novel resin-based dental materials. While nano silver has demonstrated excellent antibacterial potential, its application in pit and fissure sealants remains largely unexplored. The development of green synthesis methods has emerged as a promising alternative approach to synthesize metal nanoparticles using nontoxic chemicals, renewable materials, and environmentally friendly solvents. In this context, green biosynthesis of natural plants and waste eggshells offers a promising avenue for the synthesis of metal nanomaterials that can replace expensive organic polymers and surfactants and mitigate their negative impact on the environment. Our research aims to leverage green synthesis to enhance the antibacterial properties of pit and fissure sealants and evaluate their clinical application value, offering novel insights into improving the anti-caries performance of oral materials.

Materials and Methods

Antibacterial Research

Inhibition Zone Experiment

The *S. mutans* standard strain (ATCC 25175) and *L. acidophilus* standard strain (ATCC 4356) were procured from ATCC. *S. mutans* was cultured in BHI broth (Brain Heart infusion broth, Oxoid Ltd, Basingstoke, Hants, UK), and *L. acidophilus* was cultured in MARS broth (*Methicillin-resistant Staphylococcus aureus* broth, Huankai Microbial, Guangzhou, China). The bacterial suspension was uniformly spread on agar plates, and excess agar was removed by punching holes with a 1 mL spear. Sample suspensions of the control groups and eggshell/Ag groups were added to the holes. The agar plates were incubated at 5% and 37 °C for 18 h and 72 h for *S. mutans* and *L. acidophilus*, respectively. The diameters of the inhibition zones were measured and compared. The experiments were repeated three times.

Minimum Inhibitory Concentration (MIC)

The *S. mutans* and *L. acidophilus* suspension and medium were mixed at a volume ratio of 1 μL:1 mL, which was evenly divided into nine sterilizing centrifuge tubes with a volume of 2 mL per tube. The eggshell/Ag suspension was added to each tube with gradient concentrations of 0, 0.005, 0.01, 0.02, 0.04, 0.08, 0.16, 0.32, and 0.64 mg/mL. The *S. mutans* suspension was incubated at 5% and 37 °C in an orbital shaker for 18 h, while *L. acidophilus* was incubated for 72 h. Subsequently, the turbidity of the bacterial suspension in each group was observed, and 100 μL of the medium was transferred to a 96-well plate. The absorbance at 600 nm was measured using a microplate reader (Molecular Devices, USA) to determine the MIC. Three repeated wells were set for each concentration in each group, and the experiment was repeated three times.

Live/Dead Assay of Biofilms on Sealant Resins

S. mutans biofilms were incubated on the sealant specimens for 1 day. The disk specimens were washed with phosphate buffered saline (PBS) and then stained with a live/dead kit (Thermo Fisher, USA). Live bacteria with intact membranes were stained with SYTO 9 to generate green fluorescence, while impaired membranes were stained with propidium iodide to induce red fluorescence. Biofilm fluorescence was imaged with an anteverted fluorescence microscope (ZEISS, Germany). Three specimens were included in each group, and five photos were randomly taken of each specimen.

Mechanical Property of Specimens

Preparation of Specimens and Micromorphology Observation

Stainless steel metal molds were designed and customized. Eggshell/Ag was incorporated into the commercial sealant resin at mass fractions of 0 wt.%, 1 wt.%, 2 wt.% and 4 wt.%, and the mixture was slowly and evenly added to the mold. The mixture was photocured with light to prepare specimen disks and demolded. The excess edges of the disks were

trimmed, and their planes were polished according to ISO 20795–12013 standards. Disks with a diameter of 10.0 mm and a thickness of 1.0 mm were obtained. The micromorphology of specimens was observed under a scanning electron microscope (FEI CZECH REPUBLIC S.R.O., Czech Republic).

Liquidity Test

Eggshell/Ag was mixed into the commercial sealant (3M ESPE Dental Products, USA) at mass fractions of 0 wt.%, 1 wt.%, 2 wt.% and 4 wt.%, and a volume of 100 μL each was inserted with a capillary of 0.1 mm^2. The observation time was set to 10 s, 30 s and 60 s according to the clinical operation time of sealing. The capillaries were removed promptly, and the length of the liquid inside was measured and recorded for analysis. The experiment was repeated three times.

Vickers Hardness and Roughness Test

Vickers hardness was measured by a microhardness tester (Shanghai Optical Instrument factory, China). The diamond head was loaded with 25 gf and resided for 10 s. Six points on the diagonal of each sample were pressurized. The objective lens was 40×, and six rhomboid indentations were averaged as the microhardness value of the specimen.[18] The surface profilometer (Kosaka Laboratory Ltd, Japan) randomly selects the test area located at the upper, middle and lower parts of the surface. The sampling length was 0.8 mm, the measuring length was 2.0 mm, and the testing speed was 0.5 mm/s. The average Ra value is regarded as the surface roughness.

Detection of *S. mutans* Biofilm on the Surface of Specimen and Well

The sterilized disks were placed in a 24-well plate, which was incubated with medium containing 1% sucrose for 24 h. After carefully removing the disks and medium, each well was added with 1 mL of PBS, the biofilm covering the bottom and side of each well were scraped with a scraper. The solution was evenly mixed and transferred to a new 96-well plate to test the absorbance. Each specimen was fully oscillated with 10 mL medium, which was diluted and evenly applied on the agar plate for colony counting. The upper surface of the specimen incubated with the bacterial solution was carefully clamped upward into a new 24-well plate. Another group of disk incubation, 400 μL of STYO 9 fluorescence stain mixture was added to each well to soak the upper surface for 15 mins. The upper surfaces were observed under a fluorescence microscope (Nikon, Japan). Each group had 3 auxiliary wells, and each experiment was repeated three times.

Cell Culture and Identification

This study was conducted to the ethical guideline of Declaration of Helsinki and was approved by the institutional ethics committee of School and Hospital of Stomatology, Fujian Medical University. The informed consent of patients and their families, gingival tissues were cut from the edge of the third molars extractions. The HGFs cells were separated and cultured. 293T cells were ordered from the Shanghai Cell Bank of the Chinese Academy of Sciences. Cell samples were sent for Short Tandem Repeats (STR) identification, and the Polymerase Chain Reaction (PCR) Mycoplasma Detection Set was utilized to identify mycoplasma contamination. The medium was Roswell Park Memorial Institute 1640 (RPMI 1640), 10% Fetal Bovine Serum (FBS), 1% antibiotic and 0.2% mycoplasma remover.

Gradient Dilution of Extract Solution for 24 h Intervention Cells

Each sample was sterilized with ethylene oxide and immersed in cell culture medium. The surface area of specimen was 163.3 cm^2, which required 627 μL of Dulbecco's modified eagle medium (DMEM) culture containing 10% FBS according to the standards of ISO 10993–5:2009 and ISO 10993–12:2012.[19] After being placed in an incubator at 37 °C for 24 h, the medium extracts from the four groups were diluted in proportions of 1:1, 1:10, 1:100, and 1:1000. The cells were then inoculated in a 96-well plate for 24 h, and the original culture medium was replaced with 100 μL of diluted extract per well. After adding 10 μL of Cell Counting Kit-8 (CCK-8) to each well and incubating the plate at 37 °C for 1 h, the optical density (OD) value was measured at 450 nm.

Mucosal Surface Contact Experiment of Golden Hamsters

The mucosal contact experiments, which were carried out in accordance with the guidelines for the care and use of human specimens and animals, were approved by the Animal Care and Use Committee of Fujian Medical University. Twenty-four male hamsters aged 10 weeks with healthy cheek pouch mucosa were selected. The hamsters were randomly and evenly divided into four groups. The perforated specimen was sutured and fixed with medical 5–0 suture on the right cheek pouch mucosa of the hamsters after they were anesthetized by intra-abdominal injection. The suture strength was adjusted to ensure that the specimen was tightly attached to the mucosa without compression. After two weeks, the golden hamsters were sacrificed under painless anesthesia, and the samples were removed. 2 mL of blood was collected from the orbit, and the cheek pouches around the sutured specimen, liver, and kidney tissue were collected and fixed in 4% paraformaldehyde for 24 h. The tissue was then stained with hematoxylin-eosin (HE) staining and scored by two histopathologists in accordance with ISO10933 for microscopic stimulation of mucosal tissue. Next, 200 μL of blood was quickly added to 0.5 mL of 65% HNO_3 for a dark brown reaction at 60 °C for 24 h. An inductively coupled plasma mass spectrometer (ICP–MS) was used for detection with a wavelength scanning program, with the measurement being repeated three times for each sample and the average value taken. Additionally, 1 mL of blood was placed in a water bath at 37 °C for 15 mins and centrifuged at 3000 r/min for 10 mins to obtain at least 300 μL of serum. An automatic biochemical analyzer was used to determine the indices of hepatocyte injury in serum, including aspartate transaminase (AST) and alanine transaminase (ALT), liver synthesis function indicators, such as total protein (TP), albumin (ALB), and globulin (GLB), and renal function indicators, including blood urea nitrogen (BUN) and serum creatinine (CRE).

Results

Inhibitory Effects of Eggshell/Ag on *S. mutans* and *L. acidophilus*

In our previous article,[20] we reported on the synthesis and characterization of eggshell/Ag and its antibacterial properties against *S. aureus* and *E. coli*.

As demonstrated in Figure 1A and B, previously cloudy bacterial solution became clear once the concentration of eggshell/Ag reached 0.08 mg/mL in *S. mutans* solution and 0.02 mg/mL in *L. acidophilus* solution. The MICs for *S. mutans* and *L. acidophilus* and were determined to be and, respectively, by measuring the absorbance changes and plotting them on the corresponding graphs. Subsequent incubation produced obvious inhibition zones around the eggshell/Ag samples on the *S. mutans* and *L. acidophilus* agar plates. In contrast, the control groups of pure eggshell or eggshell treated with Platyphelus orientalis extract did not exhibit antibacterial function, and bacteria were found to grow normally around the control holes (Figure 1C–F). Moreover, under the microscope, *S. mutans* and *L. acidophilus* in the control groups displayed a large amount of green fluorescence and a small amount of red fluorescence, while the eggshell/Ag groups exhibited the opposite (Figure 1G–J). Additionally, SEM observations (Figure 1K and L) showed that untreated *S. mutans* appeared smooth and spherical or ovoid, with cells connected end to end in long or short chains. After eggshell/Ag treatment, the surface became rough and presented an irregular, wrinkled shape. In Figure 1M and N, normal *L. acidophilus* appeared elongated with a circular end, while eggshell/Ag treatment caused the thallus to become distorted and even shrink into a short rod shape, with cell contents leaking and blurring the surface morphology of the nanomaterials. These results indicate that eggshell/Ag directly destroys the bacterial cell wall and membrane, causing the bacterial structure to deform or disintegrate, ultimately leading to a significant antibacterial effect.

Mechanical Properties of Pit and Fissure Sealant

After testing the fluidity of the four sealant groups with Eggshell/Ag, no significant differences were found among the intervals of 10 s (F=0.7478, P=0.5363), 30 s (F=2.717, P=0.0719), and 60 s (F=1.732, P=0.1926). The Dunnett comparison among groups also revealed no significant difference (Figure 2A–C). These results indicated that there was no significant difference in fluidity among the 0 wt.%, 1 wt.%, 2 wt.%, and 4 wt.% groups. Moreover, the four groups were cured by light and showed a deepened color in Figure 2D–G. The SEM images of the specimens from different groups showed similar surface microstructures. The microhardness and roughness values of the 0 wt.%, 1 wt.%, 2 wt.%, and 4 wt.% sealant groups are presented in Figure 2H and I with bar charts. Overall, there was no significant

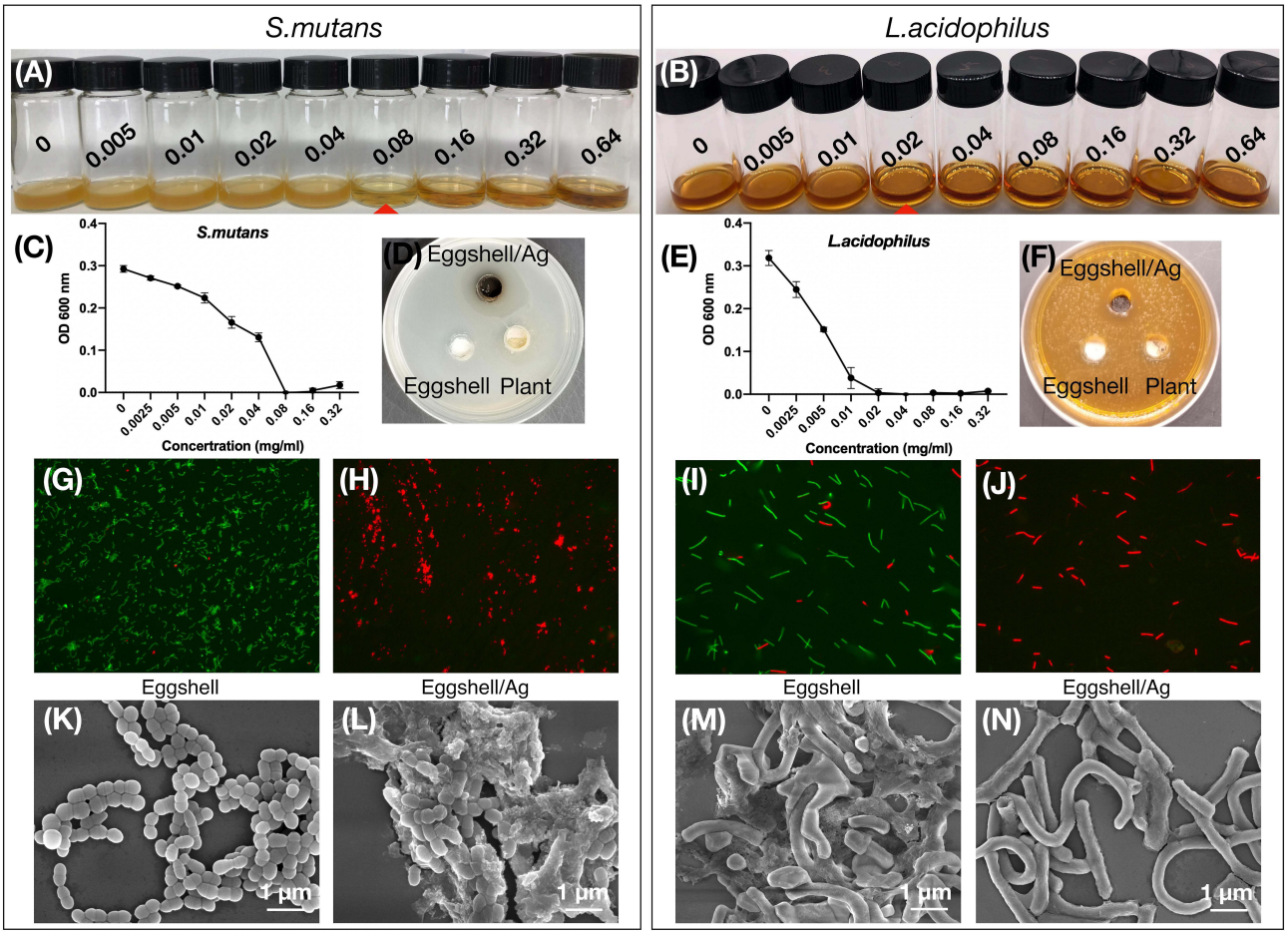

Figure 1 Inhibition effects of eggshell/Ag on *S. mutans* and *L. acidophilus*. The images and absorbance curve of *S. mutans* (**A** and **C**) *and L. acidophilus* suspension (**B** and **E**) interfered by gradient concentrations of eggshell/Ag. The inhibition zone of agar plates of *S. mutans* (**D**) *and L. acidophilus* (**F**) generated from eggshell/Ag. The merged images of fluorescence staining of *S. mutans* (**G** and **H**) *and L. acidophilus* (**I** and **J**) (×100). SEM images of *S. mutans* (**K** and **L**) *and L. acidophilus* (**M** and **N**).

difference in microhardness (F=0.6683, P=0.5948) or roughness (F=0.2506, P=0.8599), and no significant difference was observed between the groups. These findings indicated that the addition of eggshell/Ag did not lead to any significant changes in the microhardness or surface roughness of the specimens.

Effects of Specimen on *S. mutans* Bacterial Biofilm

As shown in Figure 3A–D, the fluorescence density of the *S. mutans* bacterial biofilm coating above the specimens gradually decreased with increasing eggshell/Ag concentration. Furthermore, the biofilm was blown, mixed, diluted and coated. After incubation, the colonies on the agar plates of *S. mutans* in the 1 wt.% group were slightly inhibited, while those in the 2 wt.% and 4 wt.% groups were significantly suppressed (Figure 3E–H). After removal of the specimen in each group, as shown in Figure 3I, the 24-well plate was observed and compared. In the ctrl group, the dish was completely covered by biofilm. In the 0 wt.% group, there was no biofilm in the center of the well where the specimen was placed, but the surrounding area was covered by biofilm. The 2 wt.% group showed obviously decrease in biofilm density than that in the 1 wt.% group. In the 4 wt.% group, the dish was completely clear without visible biofilm. Thereafter, the bacterial biofilm attached to the bottom of each well was scraped off and suspended in PBS. The absorbance of the suspension in Figure 3J was consistent with the abovementioned results. The OD values and growth curve of the 1 wt.%, 2 wt.% and 4 wt.% groups gradually decreased compared with the ctrl group, and the difference was statistically significant (F=259.0, P<0.001). To conclude, 0 wt.%, 1 wt.%, 2 wt.% and 4 wt.% of eggshell/Ag resulted in gradually enhanced inhibition effects on *S. mutans* biofilms.

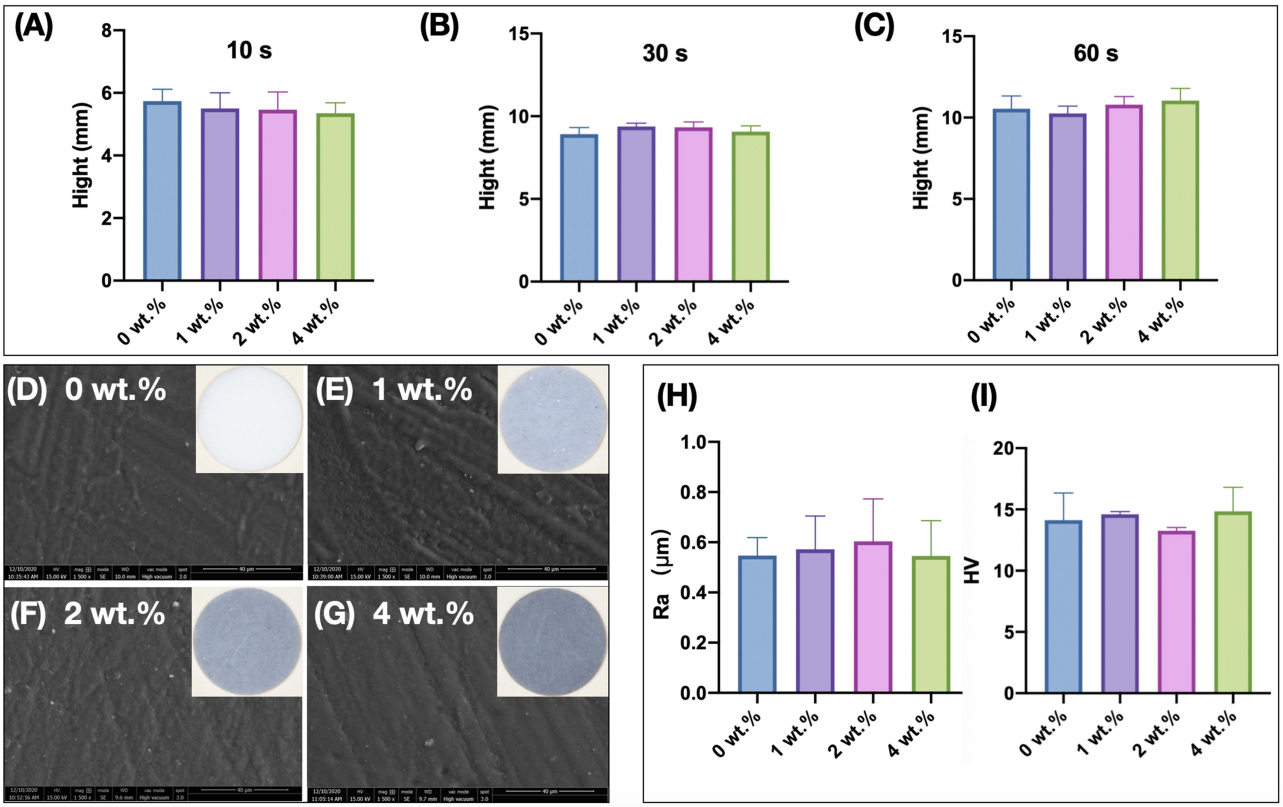

Figure 2 Mechanical properties of sealant specimens with different durations. (**A**–**C**) Height of sealant capillary siphon after 10 s, 30 s, and 60 s intervention. (**D**–**G**) Morphology and SEM images (×1500) of pit and fissure sealant specimens. (**H**) Microhardness of the specimen surfaces. (**I**) Roughness of the specimen surfaces.

HGFs Cells Were Interfered by Gradient Dilution of Sample Extract

In accordance with ISO 10993–5:2009 and other related literature,[21] gradient dilutions of sample extracts were added to HGFs and 293T cell medium to test cell cytotoxicity. After 48 h of culture, the OD value of the controlled HGF group was 0.3706 ± 0.0213. The OD values of the 0 wt.%, 1 wt.%, 2 wt.% and 4 wt.% groups gradually decreased under the 1:1 dilution, which were lower than that of the ctrl group. However, OD values in the 1:10, 1:100 and 1:1000 dilution conditions did not significantly decrease, and some groups were even higher than the ctrl group (Figure 4A). The OD value of the ctrl group was 0.77731±0.0359 after 293T cells were cultured for 24 h. The OD value of the 1:1 dilution group was significantly lower than that of the other groups, and there was no significant difference among the different groups of 1:10, 1:100 and 1:1000 dilutions and the ctrl group (Figure 4B). Microscopic observation of HGFs and 293T cells revealed that the 1:1 dilution group had fewer adherent cells, and some cells showed shrinkage and dissolution. Under the dilution conditions of 1:10, 1:100 and 1:1000, the cell morphology was normal, and there were no discrete particles in the cytoplasm or cell lysis. In conclusion, the 1:1 dilution of the extract displayed strong cytotoxicity, while the 1:10, 1:100 and 1:1000 dilutions showed weak cytotoxicity.

Animal Research

After administering anesthesia, a perforating disk was securely sutured onto the cheek pouches of Golden Syrian Hamsters, as depicted in Figure 5A. Daily checks were conducted to ensure that the disk remained in place without any dislodgement. The hamsters were subjected to careful monitoring for adverse effects such as changes in skin, hair, eyes, mucous membrane, respiratory system, circulatory system, nervous system, limb activity, and behavior pattern. However, no significant changes were observed in any of these parameters. Moreover, the body weight of the hamsters showed a steady increase as demonstrated in Figure 5B and C.

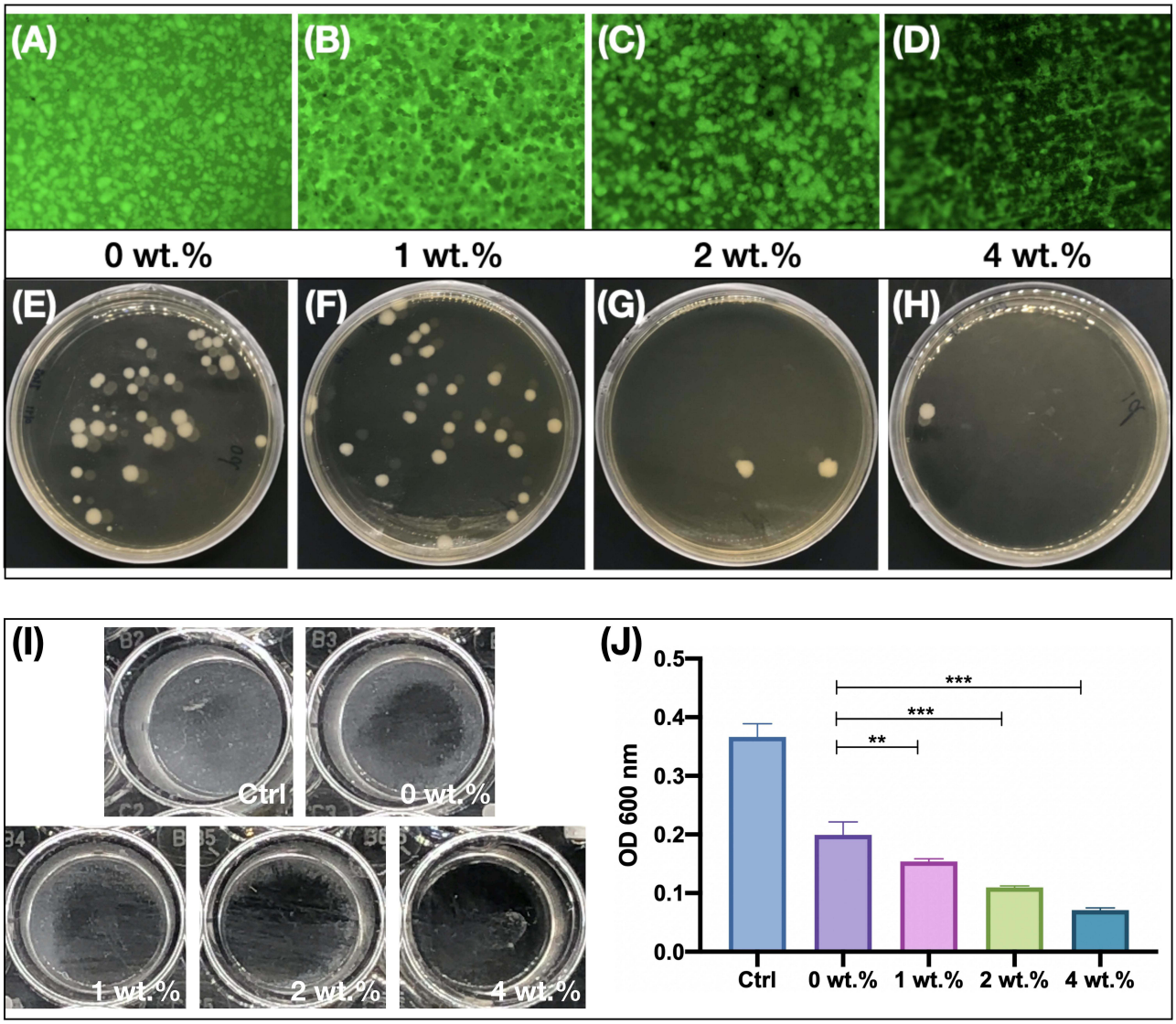

Figure 3 Inhibition of *S. mutans* biofilm formation by specimens. (**A–D**) Fluorescence staining (SYTO9, ×100) of *S. mutans* biofilms on specimen surfaces. (**E–H**) Colony count of *S. mutans* biofilms on specimen surfaces. (**I**) Images of *S. mutans* biofilms on the 24-well plates after 24 h of incubation. (**J**) OD value of biofilms of 24-well plates resuspended in solution (**: P < 0.01, ***: P < 0.001).

In the sutured groups, there were no visible indications of stimulation, injury, swelling, erosion, or ulcers in the mucosal tissues that were in direct contact with the disks except for slight hyperemia or very slight erythema. The mucosal tissue stimulation response was evaluated by two pathologists under a microscope. The epithelial keratinized layer appeared intact and clear without any cytopathic changes, tissue deformation, or erosion. Minimal leukocyte infiltration or vascular congestion was observed, and moderate to severe tissue edema was present. There was no significant difference between the two sides of the cheek pouch mucosa in the same animal, as demonstrated in Figure 5D–F. According to the oral mucosal tissue response scoring system of YY/T 0127.13–2018, the stimulation index and reaction grades were extremely mild and were shown in Table 1. When compared to the ctrl group, the histopathology of liver and kidney tissues in the 0 wt.%, 2 wt.%, and 4 wt.% sutured groups did not reveal any evident abnormalities, and there was no significant difference among the groups, as demonstrated in Figure 5G.

ICP-MS analysis revealed the absence of silver ions in the peripheral venous blood of any experimental animals, indicating that silver ions did not dissociate. The concentration of potassium ions in each group was around 2000 mg/L, indicating that the treatment did not affect potassium ions (P>0.05). Additionally, as demonstrated in Figure 5H, there

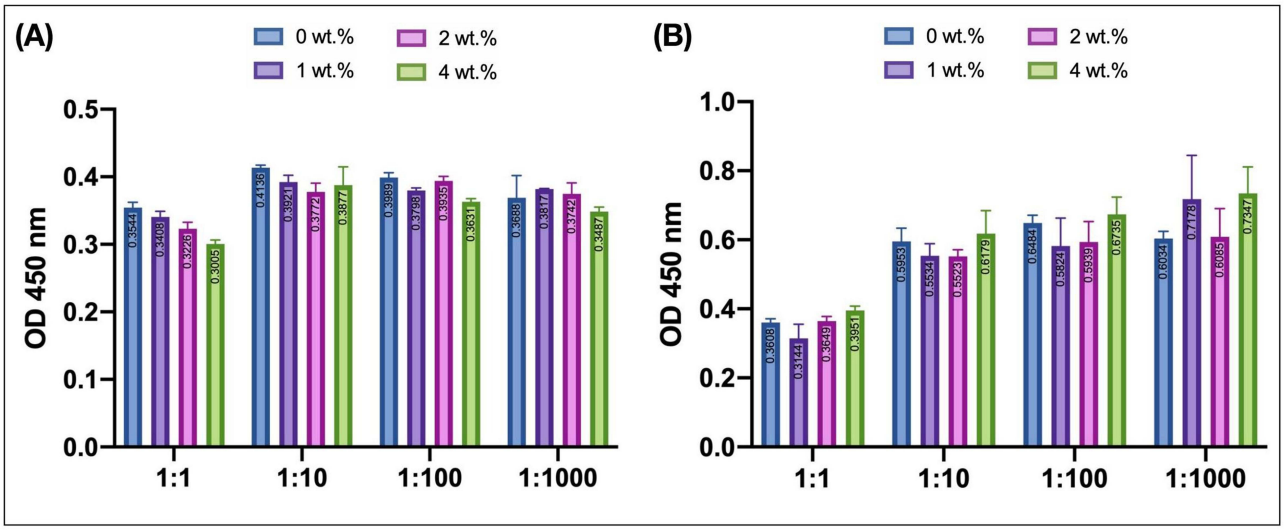

Figure 4 Cells OD values after intervention by gradient dilution of different group extracts. (**A**) OD values of HGF cell culture. (**B**) OD values of 293T cell culture.

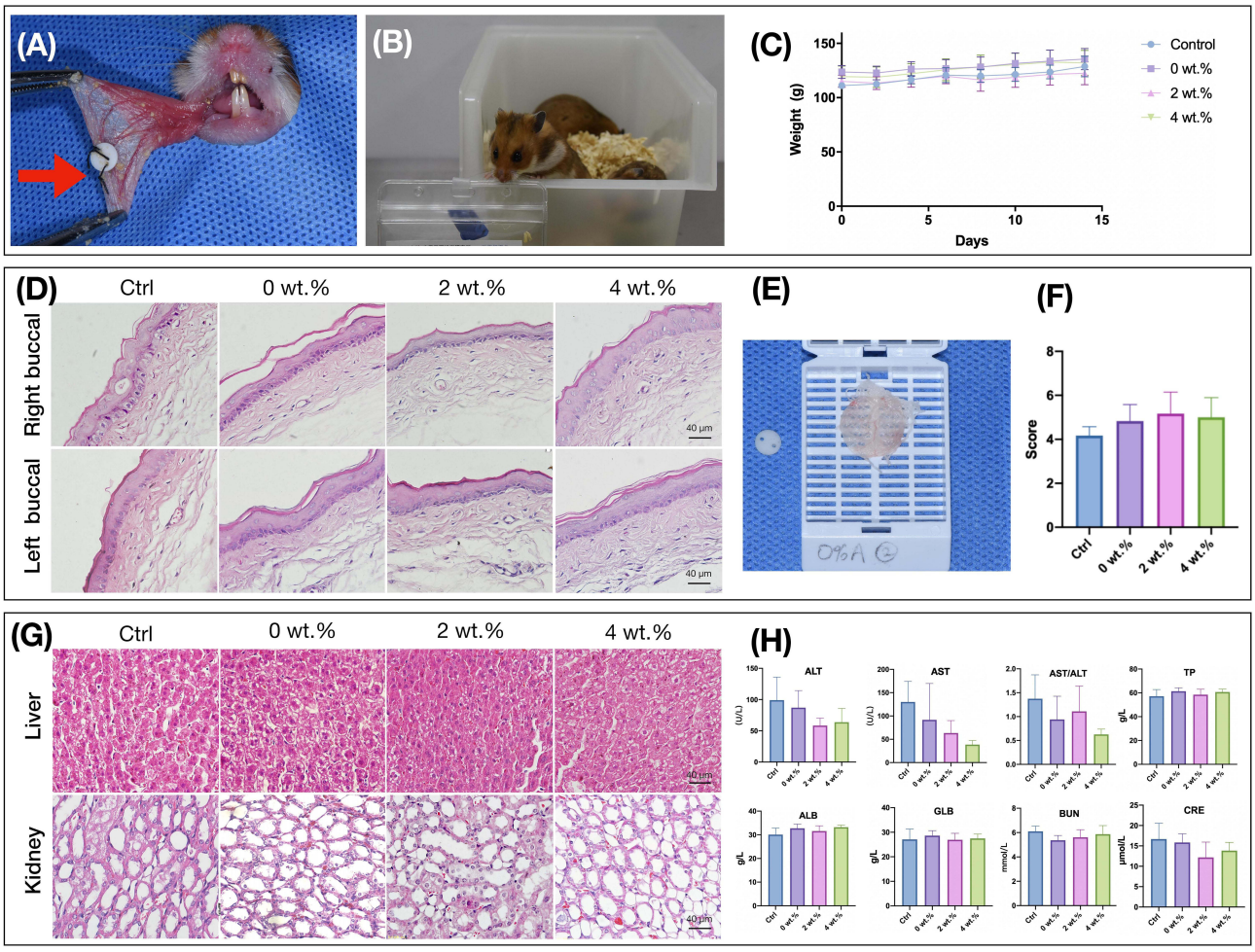

Figure 5 Cheek pouch mucosa contact test of Golden Syrian Hamster. (**A**) Punched disk sutured on the cheek pouches of the Golden Syrian Hamster. (**B**) Life status of Golden Syrian Hamster after surgery. (**C**) Growth curve of the Golden Syrian Hamster. (**D**) HE staining of cheek pouches (×400). (**E**) Resected cheek pouches contacting the disk. (**F**) The stimulation index of cheek pouches. (**G**) HE staining of liver and kidney (×400). (**H**) Liver and kidney function index of Golden Syrian Hamster.

Table 1 Stimulation Index and Response Degree of Cheek Pouches of Golden Syrian Hamster

Groups	Reaction Scores	Stimulation Index	Response Degree
Ctrl	4.17 ± 0.41		
0 wt.%	4.83 ± 0.75	0.66	Little
2 wt.%	5.17 ± 0.98	1.00	Little
4 wt.%	5.00 ± 0.89	0.83	Little

were no statistically significant differences in ALT, AST, AST/ALT, ALB, GLB, TP, or A/G among the 0 wt.%, 2 wt.%, and 4 wt.% groups, suggesting that the specimens did not have a significant influence on hepatocyte function and liver synthesis ability among all groups. Furthermore, there were no significant differences in serum BUN, CRE, or BUN/CRE among all experimental animals ($P>0.05$), indicating that there was no significant difference in renal function among the groups.

Discussion

Our research aimed to synthesize a novel sealant with extended antibacterial properties using green biosynthesis. By incorporating nano silver, the synthetic product has the potential to overcome the deficiencies of the original sealant and provide better protection against dental caries. The key to green biosynthesis is utilizing renewable eggshells and environmentally friendly plants to establish a sustainable process.

The conventional synthesis of nanoparticles involves the use of expensive organic stabilizers to prevent particle aggregation and ensure their stability on substrates. The complex synthesis processes, such as ultrasonication,[22] calcination,[23] supercritical conditions[24] and electrochemistry,[25] require the use of flammable and highly toxic chemicals, and the removal process is time-consuming, laborious, and expensive, which limits its application in many fields. Therefore, there is an urgent need for a safe and environmentally friendly method to synthesize metal nanoparticles without toxic chemicals. In recent years, the development of green synthesis processes has gained attention as an alternative method to synthesize metal nanoparticles.[26,27] The key is to establish a sustainable process using non-toxic chemicals, renewable materials, or environmentally friendly solvents.[22] Biosynthesis of metal nanoparticles utilizes natural plant extracts, is cost-effective for mass production, and the biomolecules in plant extracts are not toxic to the environment. The bioreduction process can usually be completed at room temperature, and previous studies have shown that biological molecules such as polypeptides and carbohydrates from plant extracts can serve as reducing, covering, and stabilizing agents in the synthesis of nanoparticles.[20] Biosynthesis-based Ag NPs have attracted increasing attention due to their higher stability, lower toxicity, and ease of handling and manipulation of raw materials.

It is worth noting that discarded eggshells also serve as a high-quality source of calcium and a porous carrier material. During enamel demineralization, hydroxyapatite crystals lose calcium and inorganic salts as Ca^{2+}, CO_3^{2-}, and OH^- dissociate and diffuse into the liquid phase between crystals under acid attack. Eggshells are mainly composed of calcium carbonate ($CaCO_3$, 96%), magnesium carbonate ($MgCO_3$, 1%), and calcium phosphate ($Ca_3(PO_4)_2$, 1%) crystals. In the oral saliva environment, Ca^{2+}, HCO_3-, CO_3^{2-}, OH^-, Mg^{2+}, and PO_4^{3-} from eggshell can increase local ion concentration, leading to the reversal of enamel demineralization. Additionally, Ca^{2+}, CO_3^{2-}, and OH^- can neutralize external acids and reverse the demineralization damage of enamel. Due to their environmental and biological compatibility, sustained release, and biodegradation properties,[28] eggshells have been widely used in the preparation of inorganic composite capsules, protein carriers, drugs, and nanoparticles. Studies have confirmed that silver nanoparticles can be fixed on $CaCO_3$ substrates,[29,30] and the successful application of porous silver calcium-phosphate composites has been reported.[31] The large molecular protein with functional groups inherent in eggshells can stabilize and repair Ag NPs. In some studies, eggshell/silver nanocomposites were prepared by ball milling, and their antibacterial performance was superior to that of pure silver nanoparticles. The porosity of eggshells and hydrophilic groups of protein facilitated the dispersion of nanosilver composites in aqueous solution and maximized the adhesion contact of bacteria, thereby improving their antibacterial activity.[32]

The antimicrobial activity of eggshell/Ag is potentially attributed to the presence of both silver nanoparticles and silver ions. Despite extensive discussion regarding the mechanism of action of these entities, a complete understanding has yet to be achieved.[33,34] Previous studies have suggested that silver nanoparticles and ions have a propensity to anchor and adhere to bacterial cell surfaces, resulting in perturbations to the integrity and permeability of the bacterial envelope.[35,36] Consequently, the physiological regulation of transport through the membrane and plasma is disrupted.[37,38] Cellular uptake of free silver ions has been reported to induce deactivation of respiratory enzymes and provoke high levels of reactive oxygen species, resulting in damage to the cell membrane and modification of deoxyribonucleic acid (DNA).[39] Subsequently, the compromised cell membrane structure leads to the leakage of a substantial amount of cellular contents, including ions, proteins, adenosine triphosphate (ATP), and cellular energy reservoirs.[38,40] Inside microbial cells, silver nanoparticles and ions inflict damage on cellular structures (eg, ribosomes) and biomolecules, such as DNA, lipids, and proteins.[38,41] Furthermore, they disrupt bacterial signal transduction to terminate DNA replication, the translation process in ribosomes, and protein activities, ultimately leading to cell denaturation, rupture, or even lysis.[37]

Considering the complex operation and oral environment, sealants would inevitably directly or indirectly contact the oral mucosa, and some resolvent in the saliva might enter the human body digestive system. Therefore, the development and application of new products in the human body should be evaluated and carefully based on their advantages and risks.[42] Ideally, dental materials used for permanent restoration should be chemically stable and inert in the oral environment, and the release of inorganic and organic elements from these materials has been reported. For instance, Fretwurst et al,[43] observed metallic and titanium particles in the surrounding tissues of dental implants, while synthetic resins, particularly cured methacrylate complexes, have been found to release potentially toxic chemicals, especially from cured methacrylate complexes,[44–47] which is consistent with the findings of our cell experiments. The toxicity of novel nanomaterials has been widely investigated in vitro, such as in cell experiments with dental pulp stem cell lines.[48–50] Under similar extraction conditions of Laan's cell research,[21] it was determined that the 1:10, 1:100 and 1:1000 groups had no significant inhibitory effects on HGFs and 293T cells according to ISO 10993–12 and ISO 10993–5 culture in our experiments. Although the sealant group's extract exhibited some toxicity to cells, its effects were negligible at low concentrations. Importantly, the cytotoxicity of the 1 wt.%, 2 wt.%, and 4 wt.% extracts was almost identical to that of the 0 wt.% group, suggesting that the addition of eggshell/Ag did not increase the sealant's cytotoxicity. The possible components of specimen leaching in the cell medium solution warrant further exploration and verification in future studies.

Due to the sensitive nature of the cellular environment, relying solely on cytotoxicity testing may not be sufficient to replicate the clinical setting. Therefore, additional in vitro testing is necessary to ensure the biosafety of composites. While previous studies have investigated oral NP in rodents, our research involved establishing an oral mucosal contact model in golden hamsters in accordance with ISO10933 (YY/T 0127.13–2018) to determine if the addition of eggshell/Ag had any adverse effects on local mucosa or organ function. Although some abnormalities in serum biochemical indices were observed in each group, these were likely due to the serum collection process and coagulation and hemolysis reactions. Overall, our modified specimen demonstrated a certain level of biological safety.

Conclusion

The eggshell/Ag-modified pit and fissure sealant demonstrated comparable mechanical properties and acceptable cytotoxicity in both in vitro and in vivo experiments, when compared to the clinical pit and fissure sealant. Additionally, it exhibited robust antibacterial properties against common dental caries bacterial biofilms, indicating promising prospects for broad clinical application.

Acknowledgments

The research project was supported by Natural Sciences Foundation of Fujian Province (grant number 2021J01794 and 2021J01801); Science and Technology Project of Fujian Provincial Health Commission (grant number 2021GGA053); Finance Department of Fujian Province (grant number 2021CZ01); the Open Project of Fujian Provincial Engineering Research Center of Oral Biomaterial (2021KQ01).

Disclosure

The authors declare that they have no conflicts of interest in this work.

References

1. Peres MA, Macpherson LMD, Weyant RJ, et al. Oral diseases: a global public health challenge. *Lancet*. 2019;394:249–260.
2. Bernabe E, Marcenes W, Hernandez CR, et al. Global, regional, and national levels and trends in burden of oral conditions from 1990 to 2017: a systematic analysis for the global burden of disease 2017 study. *J Dent Res*. 2020;99:362–373.
3. Wen PYF, Chen MX, Zhong YJ, Dong QQ, Wong HM. Global burden and inequality of dental caries, 1990 to 2019. *J Dent Res*. 2022;101:392–399.
4. Network GBoDC. Global burden of disease study 2019 (GBD 2019) results. Seattle (WA): Institute for Health Metrics and Evaluation; 2020. Available from: http://ghdx.healthdata.org/gbd-results-tool. Accessed May 15, 2023.
5. Wang X. The fourth national oral health epidemiological survey reports. People ‘s medical Publishing House; 2018.
6. Griffin SO, Gray SK, Malvitz DM, Gooch BF. Caries risk in formerly sealed teeth. *J Am Dent Assoc*. 2009;140:415–423.
7. Kashbour W, Gupta P, Worthington HV, Boyers D. Pit and fissure sealants versus fluoride varnishes for preventing dental decay in the permanent teeth of children and adolescents. *Cochrane Database Syst Rev*. 2020;11:CD003067.
8. Ahovuo-Saloranta A, Forss H, Walsh T, Nordblad A, Mäkelä M, Worthington HV. Pit and fissure sealants for preventing dental decay in permanent teeth. *Cochrane Database Syst Rev*. 2017;7:Cd001830.
9. Wright JT, Tampi MP, Graham L, et al. Sealants for preventing and arresting pit-and-fissure occlusal caries in primary and permanent molars: a systematic review of randomized controlled trials-a report of the American Dental Association and the American Academy of Pediatric Dentistry. *J Am Dent Assoc*. 2016;147:631–45 e18.
10. Lynch CD, Opdam NJ, Hickel R, et al. Guidance on posterior resin composites: academy of operative dentistry - European section. *J Dent*. 2014;42:377–383.
11. Lin NJ, Drzal PL, Lin-Gibson S. Two-dimensional gradient platforms for rapid assessment of dental polymers: a chemical, mechanical and biological evaluation. *Dent Mater*. 2007;23:1211–1220.
12. Lin NJ. Biofilm over teeth and restorations: what do we need to know? *Dent Mater*. 2017;33:667–680.
13. Spinell T, Schedle A, Watts DC. Polymerization shrinkage kinetics of dimethacrylate resin-cements. *Dent Mater*. 2009;25:1058–1066.
14. Sun J, Fang R, Lin N, Eidelman N, Lin-Gibson S. Nondestructive quantification of leakage at the tooth-composite interface and its correlation with material performance parameters. *Biomaterials*. 2009;30:4457–4462.
15. He M, Wang Q, Zhang J, Zhao W, Zhao C. Substrate-independent ag-nanoparticle-loaded hydrogel coating with regenerable bactericidal and thermoresponsive antibacterial properties. *ACS Appl Mater Interfaces*. 2017;9:44782–44791.
16. Yang X, Zhang C, Li A, Wang J, Cai X. Red fluorescent ZnO nanoparticle grafted with polyglycerol and conjugated RGD peptide as drug delivery vehicles for efficient target cancer therapy. *Mater Sci Eng C Mater Biol Appl*. 2019;95:104–113.
17. Hong F, Li W, Ji J, Ze X, Diao E. Nanostructured titanium dioxide (TiO(2)) reduces sperm concentration involving disorder of meiosis and signal pathway. *J Biomed Nanotechnol*. 2020;16:659–671.
18. Cadenaro M, Navarra CO, Antoniolli F, et al. The effect of curing mode on extent of polymerization and microhardness of dual-cured, self-adhesive resin cements. *Am J Dent*. 2010;23:14–18.
19. Lee JH, Jun SK, Kim SC, Okubo C, Lee HH. Investigation of the cytotoxicity of thermoplastic denture base resins. *J Adv Prosthodont*. 2017;9:453–462.
20. Huang X, Chang L, Lu Y, et al. Plant-mediated synthesis of dual-functional Eggshell/Ag nanocomposites towards catalysis and antibacterial applications. *Mater Sci Eng C Mater Biol Appl*. 2020;113:111015.
21. Van der Laan HL, Zajdowicz SL, Kuroda K, et al. Biological and mechanical evaluation of novel prototype dental composites. *J Dent Res*. 2019;98:91–97.
22. Sharififard H, Rezvanpanah E. Ultrasonic-assisted synthesis of SiO2 nanoparticles and SiO2/chitosan/Fe nanocomposite and their application for vanadium adsorption from aqueous solution. *Environ Sci Pollut Res Int*. 2021;28:11586–11597.
23. Rex R, Siddhanta S, Barman I. Role of aqueous-phase calcination in synthesis of ultra-stable dye-embedded fluorescent nanoparticles for cellular probing. *Appl Spectrosc*. 2021;75:1012–1021.
24. Dovale-Rosabal G, Rodriguez A, Espinosa A, Barriga A, Aubourg SP. Synthesis of EPA- and DHA-enriched structured acylglycerols at the sn-2 position starting from commercial salmon oil by enzymatic lipase catalysis under supercritical conditions. *Molecules*. 2021;26:1.
25. Malapit CA, Prater MB, Cabrera-Pardo JR, et al. Advances on the merger of electrochemistry and transition metal catalysis for organic synthesis. *Chem Rev*. 2022;122:3180–3218.
26. Nasrollahzadeh M, Momeni SS, Sajadi SM. Green synthesis of copper nanoparticles using Plantago asiatica leaf extract and their application for the cyanation of aldehydes using K4Fe(CN)6. *J Colloid Interface Sci*. 2017;506:471–477.
27. Phukan K, Devi R, Chowdhury D. Green synthesis of gold nano-bioconjugates from onion peel extract and evaluation of their antioxidant, anti-inflammatory, and cytotoxic studies. *ACS Omega*. 2021;6:17811–17823.
28. Liang P, Zhao D, Wang CQ, Zong JY, Zhuo RX, Cheng SX. Facile preparation of heparin/CaCO3/CaP hybrid nano-carriers with controllable size for anticancer drug delivery. *Colloids Surf B Biointerfaces*. 2013;102:783–788.
29. Ueda M, Yokota T, Honda M, et al. Regulating size of silver nanoparticles on calcium carbonate via ultrasonic spray for effective antibacterial efficacy and sustained release. *Mater Sci Eng C*. 2021;125:5.
30. Dlugosz O, Lis K, Banach M. Synthesis and antimicrobial properties of CaCO(3)-nAg and nAg-CaCO(3) nanocomposites. *Nanotechnology*. 2021;32:025715.
31. Mokabber T, Cao HT, Norouzi N, van Rijn P, Pei YT. Antimicrobial electrodeposited silver-containing calcium phosphate coatings. *ACS Appl Mater Interfaces*. 2020;12:5531–5541.
32. Apalangya V, Rangari V, Tiimob B, Jeelani S, Samuel T. Development of antimicrobial water filtration hybrid material from bio source calcium carbonate and silver nanoparticles. *Appl Surf Sci*. 2014;295:108–114.

33. Wypij M, Jedrzejewski T, Trzcinska-Wencel J, Ostrowski M, Rai M, Golinska P. Green synthesized silver nanoparticles: antibacterial and anticancer activities, biocompatibility, and analyses of surface-attached proteins. *Front Microbiol*. 2021;12:632505.
34. Yin IX, Zhang J, Zhao IS, Mei ML, Li Q, Chu CH. The antibacterial mechanism of silver nanoparticles and its application in dentistry. *Int J Nanomedicine*. 2020;15:2555–2562.
35. Khorrami S, Zarrabi A, Khaleghi M, Danaei M, Mozafari MR. Selective cytotoxicity of green synthesized silver nanoparticles against the MCF-7 tumor cell line and their enhanced antioxidant and antimicrobial properties. *Int J Nanomedicine*. 2018;13:8013–8024.
36. Liao C, Li Y, Tjong SC. Bactericidal and cytotoxic properties of silver nanoparticles. *Int J Mol Sci*. 2019;20:4.
37. Ghosh S, Patil S, Ahire M, et al. Synthesis of silver nanoparticles using Dioscorea bulbifera tuber extract and evaluation of its synergistic potential in combination with antimicrobial agents. *Int J Nanomedicine*. 2012;7:483–496.
38. Chauhan R, Kumar A, Abraham J. A biological approach to the synthesis of silver nanoparticles with Streptomyces sp JAR1 and its antimicrobial activity. *Sci Pharm*. 2013;81:607–621.
39. Ramkumar VS, Pugazhendhi A, Gopalakrishnan K, et al. Biofabrication and characterization of silver nanoparticles using aqueous extract of seaweed Enteromorpha compressa and its biomedical properties. *Biotechnol Rep*. 2017;14:1–7.
40. Li J, Rong K, Zhao H, Li F, Lu Z, Chen R. Highly selective antibacterial activities of silver nanoparticles against Bacillus subtilis. *J Nanosci Nanotechnol*. 2013;13:6806–6813.
41. Rai MK, Deshmukh SD, Ingle AP, Gade AK. Silver nanoparticles: the powerful nanoweapon against multidrug-resistant bacteria. *J Appl Microbiol*. 2012;112:841–852.
42. Handy RD, Shaw BJ. Toxic effects of nanoparticles and nanomaterials: implications for public health, risk assessment and the public perception of nanotechnology. *Health Risk Soc*. 2007;9:125–144.
43. Fretwurst T, Nelson K, Tarnow DP, Wang HL, Giannobile WV. Is metal particle release associated with peri-implant bone destruction? An emerging concept. *J Dent Res*. 2018;97:259–265.
44. Gupta SK, Saxena P, Pant VA, Pant AB. Release and toxicity of dental resin composite. *Toxicol Int*. 2012;19:225–234.
45. Hanks CT, Strawn SE, Wataha JC, Craig RG. Cytotoxic effects of resin components on cultured mammalian fibroblasts. *J Dent Res*. 1991;70:1450–1455.
46. Darmani H, Al-Hiyasat AS. The effects of BIS-GMA and TEG-DMA on female mouse fertility. *Dent Mater*. 2006;22:353–358.
47. Mousavinasab SM. Biocompatibility of composite resins. *J Dent Res*. 2011;8:S21–S9.
48. Schrand AM, Rahman MF, Hussain SM, Schlager JJ, Smith DA, Syed AF. Metal-based nanoparticles and their toxicity assessment. *Wiley Interdiscip Rev Nanomed Nanobiotechnol*. 2010;2:544–568.
49. Iavicoli I, Leso V, Bergamaschi A. Toxicological effects of titanium dioxide nanoparticles: a review of in vivo studies. *J Nanomater*. 2012;2012:1–36.
50. Mitsiadis TA, Woloszyk A, Jimenez-Rojo L. Nanodentistry: combining nanostructured materials and stem cells for dental tissue regeneration. *Nanomedicine*. 2012;7:1743–1753.